Polymer 49 (2008) 4386–4392

Contents lists available at ScienceDirect

Polymer

journal homepage: www.elsevier.com/locate/polymer

Evidences of amylose coil-to-helix transition in stored dilute solutions

Manuela Elaine Heineck [a], Mateus Borba Cardoso [a,b], Fernando Carlos Giacomelli [a], Nádya Pesce da Silveira [a,*]

[a] Bio&Macromolecular Research Group, Instituto de Química, Universidade Federal do Rio Grande do Sul, 91501-970 Porto Alegre, Rio Grande do Sul, Brazil
[b] LNLS, Laboratório Nacional de Luz Síncrotron, P.O. Box 6192, 13083-970 Campinas, Sao Paulo, Brazil

ARTICLE INFO

Article history:
Received 7 May 2008
Received in revised form 17 July 2008
Accepted 26 July 2008
Available online 8 August 2008

Keywords:
Amylose solutions
Coil-to-helix transition
Light scattering

ABSTRACT

Static (SLS) and dynamic (DLS) light scattering measurements were performed in order to study the conformational changes in amylose during storage in alkaline (KOH) and briny (KCl) aqueous solutions. Immediately after dissolution, amylose was structured as random coil and the polymer architecture was not affected by the electrolyte concentration. In stored samples the electrolyte concentration played a more important role. Although no general trend for the radii variation, depolymerisation process was not detected and an increase in the scattered light depolarization ratio was evidenced, being more pronounced for amylose chains stored in KOH. This behavior was attributed to a coil-to-helix transition in the amylose chains. Hence, the presence of precipitation after ~30 days of storage suggests the helix amylose crystallization.

1. Introduction

It is widespread known that polysaccharides generally have a tendency to aggregate in aqueous solutions which is normally caused by the huge amount of hydroxyl groups that easily lead to the formation of hydrogen bonds [1]. Depending on the quality of the solvent, this association can be shifted to high concentrations of polysaccharide where entanglements among chains are more easily detectable.

Native starch is a polysaccharide that occurs in the form of discrete and partially crystalline granules typically composed by 2 distinct macromolecules: amylose and amylopectin. Amylose is a mostly linear polymer where α-D-glycosyl units are connected by α(1,4)glycosidic linkages while amylopectin consists of highly branched chains containing α(1,4)-linked linear segments connected by α(1,6) branching points [2].

Aqueous solutions of amylose are known to be unstable and, in stored solutions, the polymer can precipitate and/or crystallize depending on the solvent nature, solution concentration as well as the molecular weight [3]. Nowadays, in order to describe these phenomena, different techniques such as rheology [4,5], ^{13}C solid-state NMR [6], small and wide-angle X-ray scattering [7–12], small-angle neutron scattering [13], infrared spectroscopy [14], Raman spectroscopy [15,16], differential scanning calorimetry [17] and electron microscopy [18–20] have been used. Nevertheless, a lack of information concerning the behavior of amylose in solution, mainly during storage in different solvents, remains to be explored.

Besides the above-described techniques, it is well-known that light scattering analysis can provide fruitful informations about polymers in solutions, and studies concerning the starch components have been reported [21–24]. However, the preparation of true solutions of polysaccharides is notoriously difficult and light scattering studies suggest that amylose solutions are often contaminated with amylopectin, amylose aggregates or impurities such as dust [25–27]. Recently, amylose fractions were characterized by means of light scattering after extraction from starch during aqueous leaching at different temperatures [28]. Studies were also devoted to investigate amylose structure by high-performance size exclusion chromatography (HPSEC) coupled with multi-angle laser light scattering (MALLS) [21,23,29]. Therefore, the goal of this work was to give some insights about the behavior of amylose chains during storage in different aqueous media using classical light scattering techniques. The methodological basis involved amylose solubilization in alkaline media and later storage in aqueous solutions containing distinct amounts of KOH or KCl. Molecular weight (M_w), radius of gyration (R_g), hydrodynamic radius (R_h), structure-sensitive parameter (ρ) and second virial coefficient (A_2) were determined through static (SLS) and dynamic (DLS) light scattering measurements in different steps of the study. Depolarized light scattering procedure was also employed in order to confirm the coil-to-helix transition in stored amylose solutions.

* Corresponding author. Tel.: +55 51 3308 7321; fax: +55 51 3308 7304.
E-mail address: nadya@iq.ufrgs.br (N.P. da Silveira).

0032-3861/$ – see front matter © 2008 Elsevier Ltd. All rights reserved.
doi:10.1016/j.polymer.2008.07.062

2. Experimental section

2.1. Samples preparation

Commercial amylose (Sigma) was dissolved in 5 mol L^{-1} KOH solutions and stirred overnight. Afterwards, the solutions were diluted using water or HCl in order to obtain KOH and KCl solutions with different concentrations. Amylose solutions were then filtered through 1.20 and 0.45 μm pore membranes and placed into dust free cells for light scattering measurements.

2.2. Light scattering measurements

Light scattering measurements were carried out on an automatic BI-200M goniometer and a BI-9000 AT digital correlator (Brookhaven Instruments). A coherent He–Ne laser ($\lambda = 632.8$ nm) was used as light source. All solutions were thermostated in a refractive-index-matching liquid (decalin) at room temperature (20 °C). SLS and DLS measurements were performed in triplicate at different scattering angles within the range of $30° < \theta < 150°$. Depolarized light scattering measurements were performed using a Glann-Thompson prism having an extinction ratio better than 10^{-7} which was placed before the entrance of the detector. The scattered light was collected in I_{VV} (same direction of the polarized incident beam) or in I_{VH} (normal direction related to the polarized incident beam) geometries. The well-known depolarization ratio of benzene ($I_{VH}/I_{VV} = 0.26$) was used as standard in order to verify the correct position of the prism.

2.3. Analysis of SLS data

2.3.1. Zimm plot

This is a useful method that allows us to have preliminary characteristics from polymer solutions, in which the average scattering intensity is related to the macromolecular properties through the relation described as:

$$\frac{Kc}{R_\theta} = \left[1 + \frac{R_g^2 q^2}{3}\right]\left(\frac{1}{M_w} + 2A_2 c\right) \tag{1}$$

wherein the concentration c is expressed in mg mL^{-1}. K is the optical contrast expressed by the equation:

$$K = \frac{4\pi^2 n^2 \left(\frac{dn}{dc}\right)^2}{N_A \lambda^4} \tag{2}$$

and R_θ (Rayleigh ratio) is the normalized scattered intensity (toluene was applied as standard solvent). Moreover, n is the refraction index of the solvent and dn/dc is the refractive index increment. The scattering vector (q) is given by Eq. (3).

$$q = \frac{4\pi n}{\lambda}\sin\left(\frac{\theta}{2}\right) \tag{3}$$

Thus, from the plot of Kc/R_θ vs. $q^2 + kc$ and extrapolating to zero angle and concentration, the values of R_g and A_2 can be obtained from the slopes and M_w is extracted from the inverse of the intercepts.

2.3.2. Dissymmetry method

This method was used to determine R_g of the polymer chains during storage, in the following way [30]:

$$d(\theta) = \frac{I(\theta)}{I(180-\theta)} \approx 1 + \left(\frac{4\pi}{\lambda}\right)^2 \left(\frac{R_g^2}{3}\right)\cos\theta \tag{4}$$

The scattered light was collected in complementary angles and its ratio was plotted against $\cos\theta$. Thus, the linear slope of the curve gives R_g of the scattering objects.

2.4. Analysis of DLS data

In a DLS experiment, the time-dependent fluctuations in the scattered intensity due to the random thermal motion of the particles are analyzed using a digital correlator and processed as an autocorrelation function [31]. Normalized electric field autocorrelation functions $g_1(t)$, calculated from $g_2(t)$ were analyzed using the program GENDIST which employs the algorithm REPES to perform the inverse Laplace transformation as demonstrated in Eq. (5), [32].

$$g_2(t) - 1 = \beta\left[\int A(\tau)\exp(-t/\tau)d\tau\right]^2 \tag{5}$$

wherein t is the delay time of the correlation function and β is an instrumental parameter. The resulting $A(\tau)$ is a distribution of relaxation times that consist generally of several peaks representing individual dynamic processes. Herein, the distributions of the relaxation times are shown in the equal area representation [33] as $\tau A(\tau)$ vs. $\log\tau$.

The mean relaxation time τ or the relaxation frequency Γ (τ^{-1}) characteristic of a dynamic process can be quantitatively associated to an apparent diffusion coefficient (D) determined according to the relation:

$$D = \frac{\Gamma}{q^2} \tag{6}$$

Finally, the hydrodynamic radius (R_h) is derived from the diffusion coefficient (D) using the well-known Stokes–Einstein relation:

$$R_h = \frac{k_B T}{6\pi\eta D} \tag{7}$$

k_B is the Boltzmann constant, T is the absolute temperature and η is the viscosity of the solvent.

3. Results and discussion

3.1. Preliminary characterization

SLS measurements were performed in 0.1 mol L^{-1} KOH solutions to obtain elementary macromolecular characteristics of amylose. The values of M_w, A_2 and R_g were determined from Zimm plot (depicted in Fig. 1) and are listed in Table 1.

The same M_w value (1.69×10^5 g mol^{-1}) was obtained independent of the considered extrapolation (with associated error of ±1.9% for both extrapolations – concentration and angular dependencies). It is difficult to compare the determined M_w with those ones found in the literature since the amylose synthesis is rather complex allowing to a wide range of molecular weight depending on the botanical source. However, it was possible to find similar values throughout the literature [34]. It is worth to mention that the tendency of aggregation in polysaccharides makes difficult the accurate determination of their molecular weight by means of SLS [35]. It came from the fact that SLS is a tremendously sensitive technique towards high molecular components (large aggregates for example) and even a very small number of large particles can lead to a pronounced contribution in the total average scattering intensity. However, as discussed hereafter, the determined M_w value is reliable and it has no interference of aggregates. The value is related only to the molecular weight of one single polymer chain.

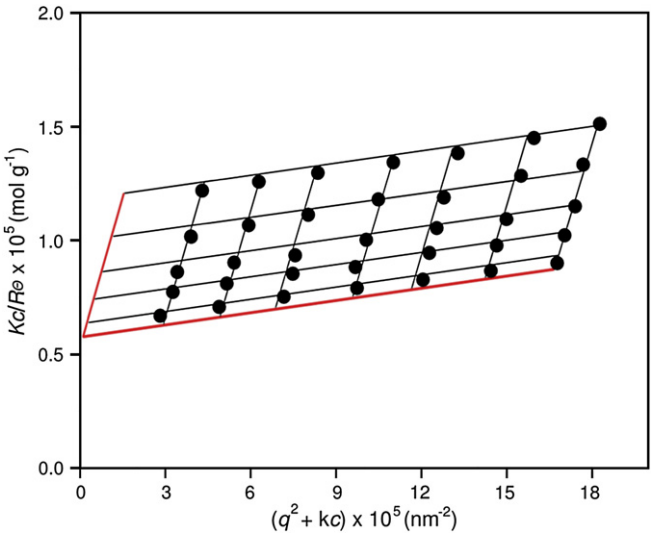

Fig. 1. Zimm Plot acquired from amylose dissolved in KOH 0.1 mol L^{-1}.

The A_2 and R_g values were found to be 9.71×10^{-4} cm^3 mol g^{-2} and 62.5 nm, respectively.

Fig. 2A shows the autocorrelation functions monitored at different angles for 1.0 mg mL^{-1} amylose in 0.1 mol L^{-1} KOH solution. Autocorrelation functions are observed to decay faster whilst the scattering angle is increased. Fig. 2B represents the characteristic distributions of relaxation times. No significant changes were observed and the single distribution was slightly displaced to higher values of log τ when the scattering angle was shifted to smaller values. Fig. 2C depicts the q^2 dependence of Γ. The width line of the characteristic relaxation frequency was q^2 dependent and the extrapolation to $q \to 0$ crossed the origin suggesting a diffusional dynamic process.

Table 1 also lists the apparent diffusion coefficient ($D = 6.05 \times 10^3$ nm^2 s^{-1}) obtained from the slope of Γ vs. q^2 and the apparent hydrodynamic radius ($R_h = 38.4$ nm) determined using the Stokes–Einstein relation. Similar values of D were found for all other solutions measured suggesting that the diffusion rate of amylose coils was concentration independent since all analyzed solutions (concentration of amylose smaller than 2 mg mL^{-1}) were at the dilute concentration regime. Critical overlap polymer concentration (c^*) was calculated according to the relation [36]:

Table 1
Molecular properties of the commercial amylose used in the experiments

Parameter	Values
M_w (g mol^{-1})	1.69×10^5
A_2 (cm^3 mol g^{-2})	9.71×10^{-4}
R_g (nm)	62.5
D (nm^2 s^{-1})	6.05×10^3
R_h (nm)	38.4
c^* (mg mL^{-1})	6.1
ρ	1.6

$$c^* = \frac{1}{A_2 M_w} \tag{8}$$

A c^* value of 6.1 mg mL^{-1} was determined (also in Table 1). The dilute regime was also confirmed by the absence of slow modes in the curves displayed in Fig. 2B.

The static and hydrodynamic dimensions vary with the macromolecular structure and a combination of both may provide qualitative informations about the architecture of the macromolecules. This can be done from the values of the structure-sensitive parameter (ρ) which is defined by the ratio between R_g and R_h [37]. ρ values for different molecular architectures can be found elsewhere [38]. Generally, ρ decreases when branching density increases. On the other hand, an increase in polydispersity counteracts the effect of branching. At 20 °C, the ρ value for amylose chains dissolved in 0.1 mol L^{-1} KOH solutions was found to be 1.6 (Table 1). It is higher than the predicted for a homogeneous hard sphere (0.79) and compatible with a monodisperse random coil of linear chain.

3.2. Amylose storage analysis

Scheduled measurements were performed from a series of 1.0 mg mL^{-1} amylose solutions during storage. Fig. 3 depicts R_h and R_g for amylose dissolved in KOH solutions and stored for up to 12 days.

As can be seen in Fig. 3A, the value of R_h is quite independent of KOH concentration in the unstored samples. Instead, a general reduction was observed when the samples were stored and the effect was enhanced for the smallest amounts of KOH. The value of R_g was also concentration independent in unstored samples (Fig. 3B). A slight reduction was observed for shorter periods of storage depending on the KOH concentration and, from this point

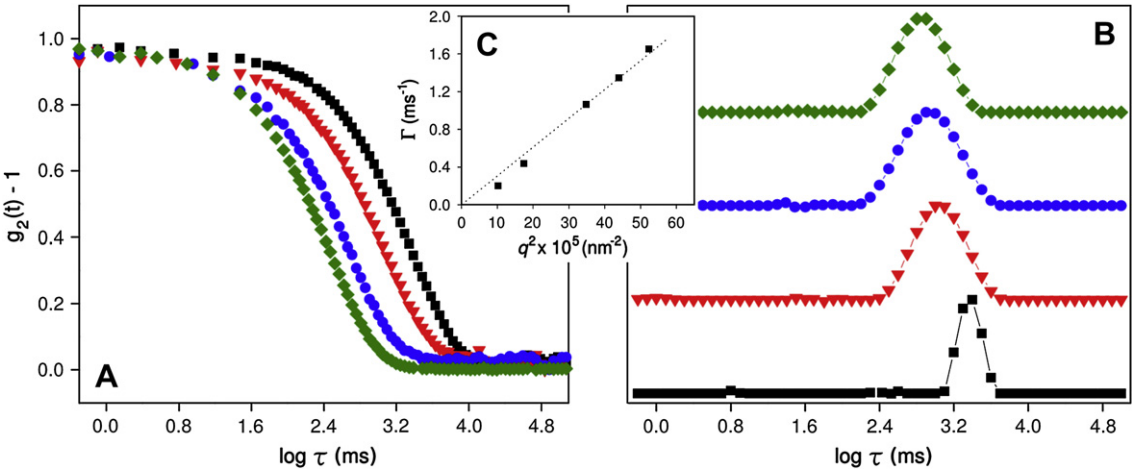

Fig. 2. Autocorrelation functions (A) and distribution of relaxations times (B) from a 1.0 mg mL^{-1} amylose solution in 0.1 mol L^{-1} KOH solution when DLS was performed at different scattering angles: 45° (■), 60° (▼), 90° (●) and 120° (◆). The inset (C) depicts the q^2 dependence of Γ.

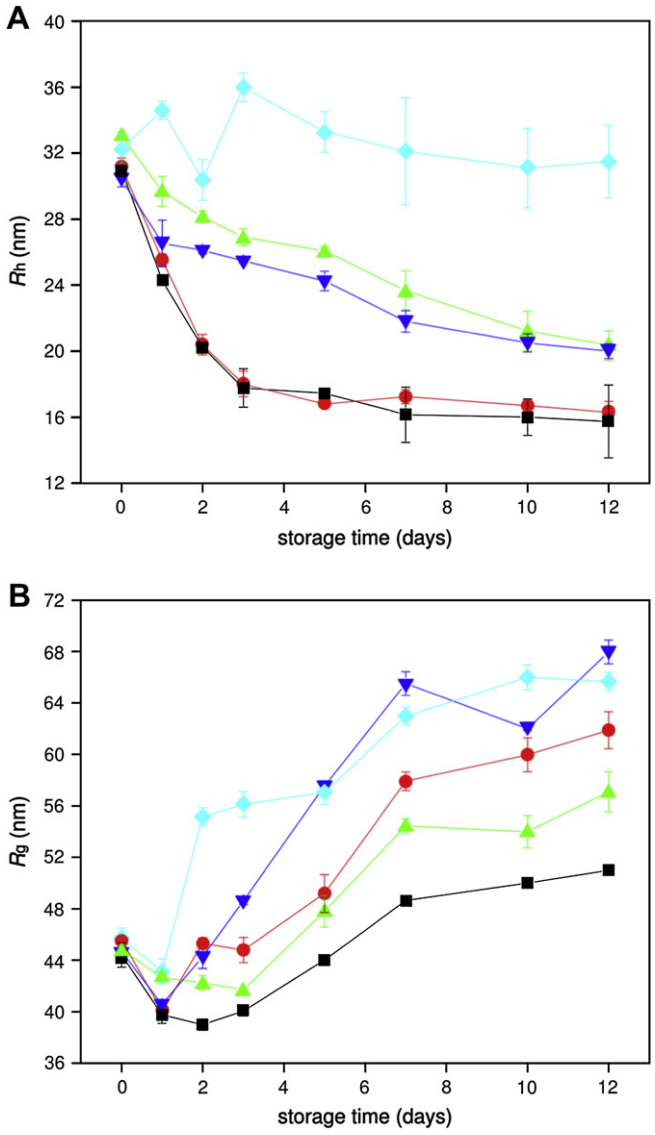

Fig. 3. Influence of storage time and KOH amount in R_h (A) and R_g (B) values of amylose chains in alkaline aqueous solutions. KOH concentrations: 0.8 (■), 1.0 (●), 1.2 (▲), 1.4 (▼) and 1.8 (◆) mol L^{-1}.

onward, R_g increased sharply. A reduction of R_h, together with an increase in R_g, may be associated to the appearance of a stiffed chain. Table 2 portrays the ρ values calculated from the determined radii values. Depending on the KOH concentration, this ratio increases with the storage from roughly 1.4 (classical random coil structures) to values as high as 3.7.

The same procedure was employed to study amylose behavior in briny solutions. Fig. 4 depicts the influence of storage in R_h and R_g values of amylose chains in KCl aqueous solutions with different concentrations.

Following the same trend reported in alkaline media, the values of R_h (Fig. 4A) and R_g (B) were KCl concentration independent in unstored samples. In stored samples, R_h values displayed different contraction tendencies. In high concentrated KCl solutions (1.4 and 1.8 mol L^{-1}), a R_h value ~22 nm was determined in unstored samples. This value was reduced to roughly 8 nm after 12 days. On the other hand, in dilute KCl solutions (0.8 and 1.0 mol L^{-1}) R_h values decreased slower. R_g values were smaller than those measured in KOH. According to the previous results, corn amylose dissolved in water or DMSO also has smaller dimensions than the ones obtained in alkaline media [39,40]. However, it was possible to

Table 2
Structure-sensitive parameter (ρ) values for amylose dissolved in KOH aqueous solutions with different concentrations as function of storage time (average of 3 measurements; standard deviation – SD ≤ 0.1)

KOH (mol L^{-1})	Storage time (days)					
	Unstored	3	5	7	10	12
0.8	1.4	2.2	2.5	3.0	3.1	3.4
1.0	1.6	2.5	2.9	3.3	3.6	3.7
1.2	1.4	1.5	1.8	2.3	2.5	2.8
1.4	1.5	1.9	2.4	2.7	2.9	2.9
1.8	1.4	1.5	1.7	1.9	2.1	2.1

observe a reduction in R_g values for longer storage times, for solutions having high amounts of KCl. A special feature took place in the solutions containing 1.2 mol L^{-1} of KCl, where amylose dimensions remained almost constant during storage probably due to the balance of charges between the polymer and the solvent. This amount of KCl seemed to be adequate to stabilize the chains without significant size variations during a short storage time.

The values of the structure-sensitive parameter ρ for amylose–KCl solutions are given in Table 3. The ratio increased with storage

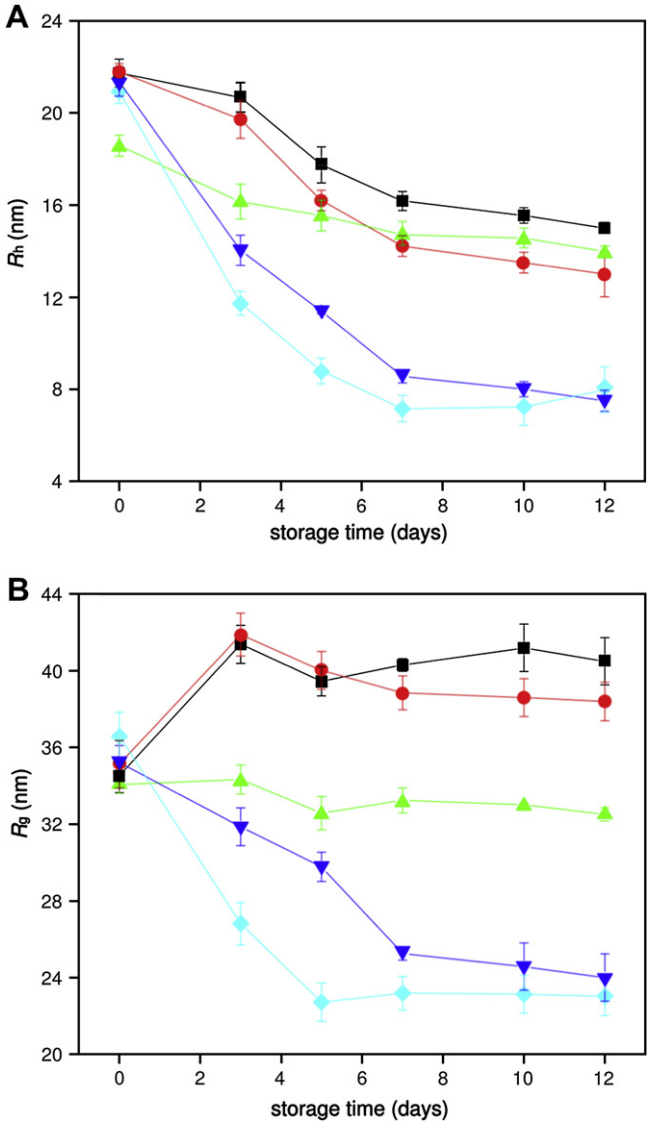

Fig. 4. Influence of storage time and KCl amount in R_h (A) and R_g (B) values of amylose chains in briny aqueous solutions. KCl concentrations: 0.8 (■), 1.0 (●), 1.2 (▲), 1.4 (▼) and 1.8 (◆) mol L^{-1}.

Table 3
Structure-sensitive parameter (ρ) values for amylose dissolved in KCl aqueous solutions with different concentrations as function of storage time (average of 3 measurements; standard deviation – SD $\leq$ 0.1)

KCl (mol L^{-1})	Storage time (days)					
	Unstored	3	5	7	10	12
0.8	1.6	2.0	2.2	2.5	2.6	2.7
1.0	1.6	2.1	2.5	2.7	2.8	2.9
1.2	1.8	2.1	2.1	2.3	2.3	2.3
1.4	1.6	2.3	2.6	2.9	3.0	3.2
1.8	1.7	2.0	2.4	3.1	3.1	3.1

time suggesting changes in the coil structure. The values ranged from 1.7 in unstored samples to ~3.2 after 12 days. This evolution of ρ values was less pronounced if compared with the rate in KOH solution at 0.8 mol L^{-1} (Table 2). As it was expected, the small variation of the radii in 1.2 mol L^{-1} KCl solution led to the smallest increase of ρ. The time dependence variation in ρ for the smallest concentration of both electrolytes is also depicted in Fig. 5 in order to give a better visualization of the phenomenon.

Initially, it was supposed that these changes could be linked to aggregation processes and/or polymer degradation. The first hypothesis was excluded since the emergence of secondary slow modes or displacement of the single distribution was not revealed by REPES analysis even after 12 days of storage. As well, a process of depolymerisation (polymer degradation) during storage, related to hydrolysis of amylose chains, seemed not to happen once it would generate quicker-diffusive species and they would be seen as a new structural contribution in the distributions of relaxation times, which was never observed. Moreover, a possible process of degradation was also checked by means of Benedict's test in order to monitor reducing sugar presence [41,42]. Benedict's solution is a light blue solution that in the presence of reducing sugar and under heat leads to the formation of a red precipitate containing cuprous oxide (red/brown color). Fig. 6 shows bottles containing Benedict's pattern and solutions of amylose and glucose after performed the mentioned test. A typical pure Benedict's solution is depicted on Fig. 6A while (B) is an amylose solution stored for 12 days where the light blue color is seen. The red/brown color observed in standard glucose solutions (Fig. 6C and D) evidences a positive test where the presence of reducing sugar is confirmed. All amylose solutions under heat and in the presence of the Benedict's solution showed undoubtedly light blue color as in Fig. 6B.

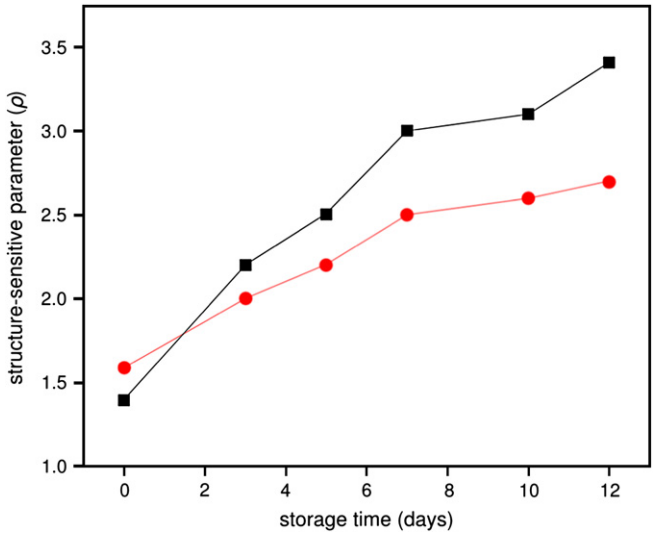

Fig. 5. Time dependence of ρ for the smallest concentration of electrolyte used (0.8 mol L^{-1}): KOH (■) and KCl (●).

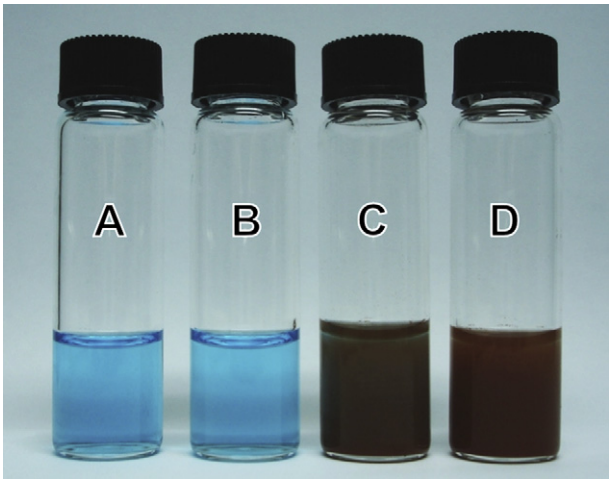

Fig. 6. Benedict's test performed to verify the presence of glucose. (A) Benedict's solution (light blue color); (B) 1.0 mg mL^{-1} amylose solution in 1.8 mol L^{-1} KCl stored for 12 days (light blue color); (C) 1 mg mL^{-1} (red/brown color) and (D) 0.5 mg mL^{-1} (red/brown color) glucose standard solutions.

These observations suggest the total absence of free glucose during the whole storage period excluding the possibility of a depolymerisation process.

Thus, the experimental results have their origin associated to changes in the structure of amylose chains during storage. From DLS, the slump observed in R_h values is believed to be related to a reduction in the polymer–solvent affinity. As amylose was dissolved in concentrated alkali aqueous solutions, the hydrogen bonds responsible for the helix conformation in bulk were progressively disrupted and the chains adopted a random conformation. In pH 12, the helical conformation was supposed to be completely absent as it was already viewed experimentally [34] and confirmed by the ρ parameter calculated herein in unstored samples. Nonetheless, when solutions were stored, intramolecular interactions were supposed to be progressively replaced leading to a reduction on the volume of the free chains, connected to a reduction in polymer–solvent interaction. Furthermore, the intramolecular affinity between units of the amylose chains promotes changes on R_g values noticed by the alterations in the polymer conformation (ρ values). Bello-Perez et al. [43] reported a similar effect considering ρ values determined during storage of amylose in KCl solutions.

Fig. 7 shows the schematic representation of amylose conformation evolution during storage. It is suggested that the increase in the values of the sensitive parameter ρ is related to a transition from a monodisperse random coil to a helix amylose chain conformation that is progressively formed during storage.

According to Burchard [38], the value of ρ for a rigid rod, consistent with a helix structure, is proportional to:

$$\rho = \frac{\sqrt{3}}{3} \ln N \tag{9}$$

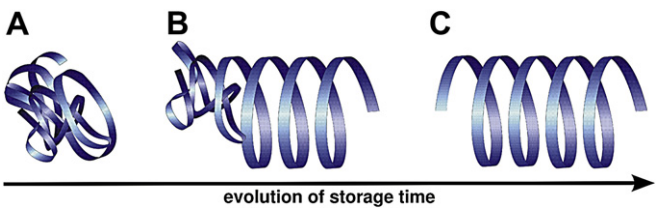

Fig. 7. Schematic representation of amylose conformation evolution during storage. (A) Monodisperse random coil; (B) intermediate conformation between monodisperse random coil and helix state; (C) amylose helix.

wherein, N is the number of repeating units. Considering M_w determined using Zimm plot and the molar mass of the glycosyl unit (162 g mol^{-1}), the degree of polymerization of the used amylose is around 1000. Thus, bearing in mind that the chains are changing their conformation to a helix, ρ should achieve values around 4.0 for infinite storage time. We determined values up to 3.7, supporting this idea.

The suggested transition is also sustained by the depolarization ratio (I_{VH}/I_{VV}) determined from 1.0 mg mL^{-1} amylose solution in 0.1 mol L^{-1} KOH during storage (Fig. 8). The depolarization ratio rose from a mean value of 6.0×10^{-3} (unstored sample) to 8.3×10^{-3} (12 days of storage). It clearly suggests the formation of a rigid structure such as a helix. In addition, after approximately 5 days of storage, the scattering intensity coming from the solution (I_{VV} and I_{VH}) decreased related to the beginning of amylose precipitation. However, up to 12 days of analysis no significant precipitate was seen on the bottom of the scattering cuvettes by the naked eye.

In KCl solutions, the helix formation also took place within a lower-rate, which can be seen clearly in Fig. 5. The slope of the increment in ρ vs. storage time is more pronounced in KOH than in KCl comparing solutions with the smallest amount of electrolyte (0.8 mol L^{-1}). Unfortunately, it was not possible to monitor the increase in the depolarization ratio in KCl solutions since the fraction of depolarized light intensity coming from the solutions was not sufficiently high to be precisely detected in the I_{VH} geometry.

Precipitates were only observed in the bottom of the light scattering cuvettes after a long period of storage (~30 days in KOH solutions and ~60 days in KCl solutions). It matches with the reduction in the absolute scattered light since a fraction of amylose sample probably starts to precipitate after ~5 days of analysis without a visual perception. The precipitation process seems to be directly related to ρ values. As a general trend, the rate of increase in these values is qualitatively proportional to this deposition process. A progressive dropping in A_2 value was noticed for the KOH system, being equal to -1.12×10^{-4} cm^3 mol g^{-2} after 12 days of storage. It means that KOH solution does not behave as a good solvent for amylose and that the interactions of polymer–polymer are favorable. The suitable intramolecular interaction in amylose chains led to a transition in the chain conformation noticed by the constant increase in the value of ρ, and posterior precipitation.

The evidence of precipitation was also observed experimentally. The presence of slow modes in the distribution of relaxation times extracted from the autocorrelation functions was not seemed for the longest storage time monitored. However, after storage, we experimentally noticed the occasional passage of large particles in the scattering volume affecting the measurements quality. The measurements affected were excluded and new ones were acquired. Since the solutions were dust free from the beginning of the measurements (we noticed it in the measurements of unstored solutions), this behavior makes us to speculate that when the storage time is increased, large particles crossing the scattering volume are amylose crystals in a precipitation process, which are heavy to stay in solution and large for their movement to be correlated in time.

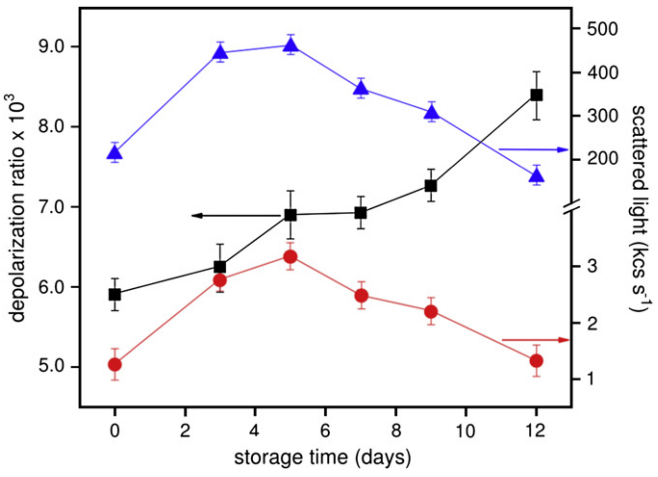

Fig. 8. Evolution of depolarization ratio (■) and scattered light collected at 90°: VH (●) and VV (▲) geometries from a 1.0 mg mL^{-1} amylose solution in 1.0 mol L^{-1} KOH during storage.

It is well-known that amylose can be recrystallized in vitro into A, B, and V crystalline lamellar forms with different morphologies. [44]. In the A structure, double helices are packed with the $B2$ space group in a monoclinic with 4 water molecules per monoclinic unit cell, while in the B structure the double helices are packed with the $P6_1$ space group containing 36 water molecules per hexagonal unit cell [45,46]. Amylose single helices (V crystalline form) are formed in dilute amylose solutions by the association with monoacyl lipids, emulsifiers and smaller ligands, such as water, alcohols or flavor compounds [44]. In the literature, V-amylose crystals have been described presenting different morphologies, space groups and sizes [47–57]. Amylose can also be recrystallized as spherulites [44,58] and fibrillar crystals [44]. It was also reported the formation of B-type double helix amylose in precipitates deposited from dilute aqueous solutions [59].

Actually the characterization of the amylose residues formed in the bottom of the cuvettes is in progress. Efforts have been devoted to study the relation between mentioned precipitate and crystallization of the amylose mainly through microscopic and diffraction techniques.

4. Conclusions

The goal of this work was to study the amylose conformational behavior as a function of storage time in different aqueous media. The chemical nature, as well as the concentration of solvents, was not able to affect the polymer chain dimensions immediately after dissolution. However, the radii of the polymer were significantly affected without any apparent general trend in stored solutions. Depolymerisation process was detected neither by Benedict's test nor by a new structural contribution in the faster region of the distribution of relaxation times. An increase in the structure-sensitive parameter ρ was observed against storage related to a coil-to-helix transition. This evidence was clearly reinforced by the results obtained from depolarized light scattering measurements and by the presence of precipitated sample after 30 days of storage.

Acknowledgements

The authors thank Fapergs, CAPES and CNPq for the fellowships granted to M.E.H., M.B.C. and F.C.G., respectively.

References

[1] Burchard W. Biomacromolecules 2001;2:342.
[2] Buléon A, Colonna P, Planchot V, Ball S. Int J Biol Macromol 1998;23:85.
[3] Putaux JL, Buléon A, Chanzy H. Macromolecules 2000;33:6416.
[4] Doublier JL, Choplin L. Carbohydr Res 1989;193:215.
[5] Clark AH, Gidley MJ, Richardson RK, Ross-Murphy SB. Macromolecules 1989;22:346.
[6] Morgan KR, Furneaux RH, Stanley RA. Carbohydr Res 1992;235:15.
[7] Miles MJ, Morris VJ, Orford PD, Ring SG. Carbohydr Res 1985;135:271.
[8] Ring SG, Colonna P, l'Anson KJ, Kalichevsky T, Miles MJ, Morris VJ, et al. Carbohydr Res 1987;162:277.
[9] l'Anson KJ, Miles MJ, Morris VJ, Ring SG, Nave C. Carbohydr Polym 1988;8:45.
[10] Gernat C, Reuther F, Damashun G, Schierbaum F. Macromolecules 1989;22:341.
[11] Manners DJ. Carbohydr Polym 1989;11:87.

[12] Cameron RE, Donald AM. J Polym Sci Part B Polym Phys Ed 1993;31:1197.
[13] Vallêra AM, Cruz MM, Ring S, Boué F. J Phys Condens Matter 1994;6:311.
[14] Goodfellow BJ, Wilson RH. Biopolymers 1990;30:1183.
[15] Bulkin BJ, Kwak K, Dea ICM. Carbohydr Res 1987;160:95.
[16] Winter WT, Kwak YT. Food Hydrocolloids 1987;1:461.
[17] Paredes-Lópes O, Bello-Pérez LA, López MG. Food Chem 1994;50:411.
[18] Harada T, Kanzawa Y, Kanenaga K, Koreeda A, Harada A. Food Struct 1991;10:1.
[19] Leloup VM, Colonna P, Ring SG, Roberts K, Wells B. Carbohydr Polym 1992;18:189.
[20] Fishman ML, Cooke P, White B, Damert W. Carbohydr Polym 1995;26:245.
[21] Fishman ML, Rodriguez L, Chau HK. J Agric Food Chem 1996;44:3182.
[22] You SG, Fiedorowicz M, Lim ST. Cereal Chem 1999;76:116.
[23] You SG, Lim ST. Cereal Chem 2000;77:303.
[24] Radosta S, Haberer M, Vorwerg W. Biomacromolecules 2001;2:970.
[25] Kodama M, Noda H, Kamata T. Biopolymers 1978;17:985.
[26] Roger P, Colonna P. Carbohydr Polym 1993;2–3:83.
[27] Cao X, Sessa DJ, Wolf WJ, Willett JL. Macromolecules 2000;33:3314.
[28] Ring SG, l'Anson KJ, Morris VJ. Macromolecules 1985;18:182.
[29] Ong MH, Jumel K, Tocarczuk PF, Blanshard JMV, Harding SE. Carbohydr Res 1994;267:99.
[30] Hellweg T, Eimer W. Colloids Surf A 1998;136:97.
[31] Berne BJ, Pecora R. Dynamic light scattering. New York: John Wiley & Sons; 1976.
[32] Jakes J. Collect Czechos Chem Communic 1995;60:1781.
[33] Štěpánek P. In: Brown W, editor. Dynamic light scattering: the method and some applications. Oxford: Oxford Science Publications; 1993.
[34] Roger P, Tran V, Lesec J, Colonna P. J Cereal Sci 1996;24:247.
[35] Praznik W, Huber A. J Chromatogr B 2005;824:295.
[36] Burchard W. In: Brown W, editor. Light scattering: principles and development. Oxford: Oxford Science Publications; 1996. p. 456.
[37] Burchard W. Macromolecules 1980;13:1265.
[38] Burchard W. Cellulose 2003;10:213.
[39] Banks W, Greenwood CT. Carbohydr Res 1972;21:229.
[40] Foster JF. In: Whistler RL, Paschall EF, editors. Starch: chemistry and technology. New York: Academic Press; 1976.
[41] Cho J, Heuzey MC, Bégin A, Carreau PJ. J Food Eng 2006;74:500.
[42] Chiou H, Fellowsa CM, Gilbert RG, Fitzgerald MA. Carbohydr Polym 2005;61:61.
[43] Bello-Perez LA, Roger P, Colonna P, Paredes-López O. Carbohydr Polym 1998;37:383.
[44] Buléon A, Véronèse G, Putaux JL. Aust J Chem 2007;60:706.
[45] Imberty A, Perez S. Biopolymers 1988;27:1205.
[46] Imberty A, Chanzy H, Perez S, Buléon A, Tran V. J Mol Biol 1988;201:365.
[47] Buléon A, Delage MM, Brisson J, Chanzy H. Int J Biol Macromol 1990;12:25.
[48] Godet MC, Tran V, Delage MM, Buléon A. Int J Biol Macromol 1993;15:11.
[49] Helbert W, Chanzy H. Int J Biol Macromol 1994;16:207.
[50] Gessler K, Uson I, Takaha T, Krauss N, Smith SM, Okada S, et al. Proc Natl Acad Sci USA 1999;96:4246.
[51] Hulleman SHD, Helbert W, Chanzy H. Int J Biol Macromol 1996;18:115.
[52] Le Bail P, Bizot H, Ollivon M, Keller G, Bourgaux C, Buleon A. Biopolymers 1999;50:99.
[53] Nuessli J, Putaux JL, Le Bail P, Buléon A. Int J Biol Macromol 2003;33:227.
[54] Nimz O, Gessler K, Uson I, Sheldrick GM, Saenger W. Carbohydr Res 2004;339:1427.
[55] Rondeau-Mouro C, Le Bail P, Buléon A. Int J Biol Macromol 2004;34:309.
[56] Le Bail P, Rondeau C, Buléon A. Int J Biol Macromol 2005;35:1.
[57] Cardoso MB, Putaux JL, Nishiyama Y, Helbert W, Hytch M, Silveira NP, et al. Biomacromolecules 2007;8:1319.
[58] Creek JA, Ziegler GR, Runt J. Biomacromolecules 2006;7:761.
[59] Gidley MJ. Macromolecules 1989;22:351.